Measurement of Region-Specific Nitrate Levels of the Posterior Chamber of the Rat Eye Using Low-Flow Push–Pull Perfusion

ARTICLE *in* ANALYTICAL CHEMISTRY · JULY 2008

Impact Factor: 5.64 · DOI: 10.1021/ac800238d · Source: PubMed

3 AUTHORS, INCLUDING:

Jeanita Pritchett
National Institute of Standards and Techn…
4 PUBLICATIONS **25** CITATIONS
SEE PROFILE

Scott Shippy
University of Illinois at Chicago
40 PUBLICATIONS **755** CITATIONS
SEE PROFILE

Anal. Chem. **2008,** *80,* 5342–5349

Measurement of Region-Specific Nitrate Levels of the Posterior Chamber of the Rat Eye Using Low-Flow Push−Pull Perfusion

Jeanita S. Pritchett,[†] Jose S. Pulido,[‡] and Scott A. Shippy*[,†]

Department of Chemistry, University of Illinois at Chicago, 845 West Taylor Street, Chicago, Illinois 60607, and Department of Ophthalmology, Mayo Clinic, 200 First Street S. W., Rochester, Minnesota 55905

The determination of the presence of nitric oxide metabolites in the rat vitreous cavity in a regioselective manner is complicated by the size and shape of the eye as well as the diffusivity of the molecule and its metabolites. In this work, in vivo low-flow push−pull perfusion sampling was utilized with a rapid capillary electrophoretic assay to monitor levels of the major NO metabolite, nitrate, at the vitreoretinal interface (VRI) of normal and aged rat models. The sampling probe tips were placed in three different positions in the posterior chamber through a 29-gauge guide needle. Sampling was performed along the VRI over the optic nerve head and regions peripheral to the optic nerve head. Additionally, samples were collected from the middle vitreous region to compare to VRI sampling. A significant ($P < 0.05$) difference in the perfusate nitrate concentration was observed in each location, which may be due to the source of NO production or the clearance mechanism of the molecule from the vitreous cavity. Infusion of L-NAME with physiological saline led to a significant decrease (35%) in the observed nitrate level. LFPPP was then utilized to observe nitrate levels after an average of 4.5 months of aging. A 3-fold increase in the mean level of nitrate over the optic nerve head was observed in mature animals compared to younger control animals. Precise measurement of NO metabolites along the VRI may provide insights into the function of NO in maintaining homeostatic conditions and the molecular changes at the diseased retina.

Nitric oxide is a diffusible inter- and intracellular messenger known to mediate several homeostatic processes.[1] In the retina, it has been demonstrated to play an important role in vasodilation,[2] neurotransmission,[3] inflammatory responses,[4] and vasculature autoregulation.[5] Retinal damage and vision deterioration associated with ocular diseases such as diabetic retinopathy,[6,7] glaucoma,[8] or those that affect the elderly population for instance, age-related macular degeneration,[9] may result from chemical imbalances such as increased NO generation. Furthermore, it has been postulated that retinal cell damage occurs in a region-specific manner in such diseases.[8,7] Due to its relatively short half-life, NO is rapidly oxidized into several end products, including its two stable metabolites nitrate (NO_3^-) and nitrite (NO_2^-).[10] Therefore, measurement of these metabolites has become an acceptable indicator of NO presence in mammalian systems.[10–13] However, since in vivo nitrite concentrations in the vitreous cavity are believed to be found at low levels ($\leq 2\ \mu M$),[14,15] which would be difficult to detect, it has become customary to assay the major metabolite, nitrate.[12] Recently, a clinical study performed in our laboratory has demonstrated elevated nitrate levels in the vitreous of patients with proliferative diabetic retinopathy.[12] Probing chemical changes in NO production via nitrate levels at the vitreoretinal interface (VRI) of an animal model could provide insights about its role in the pathology of the disease. It is therefore necessary to assay mean nitrate levels in a region-selective manner at specific locations on, or surrounding the VRI prior to subjecting animal models to conditions that would simulate retinal diseases. The measurement of NO_3^- levels at different positions in the posterior segment of the eye and over the VRI

* To whom correspondence should be addresses. Phone: (312) 355-2426. Fax: (312) 996-0431. E-mail: sshippy@uic.edu. URL: http://www.chem.uic.edu/shippy/.

† University of Illinois at Chicago.

‡ Mayo Clinic.

(1) Villani, L.; Guarnieri, T. *Brain Res.* **1996**, *743*, 353–6.
(2) Faraci, F. M.; Brian, J. E., Jr. *Stroke* **1994**, *25*, 692–703.
(3) Goldstein, I. M.; Ostwald, P. H.; Roth, S. T. *Vision Res.* **1996**, *36*, 2979–94.
(4) Nagy, G.; Clark, J. M.; Buzas, E. I.; Gorman, C. L.; Cope, A. P. *Immunol. Lett.* **2007**, *111*, 1–5.
(5) Lu, M. J.; Pulido, J. S.; McCannel, C. A.; Pulido, J. E.; Hatfield, R. M.; Dundervill lll, R. F.; Shippy, S. A. *Exp. Diabetes Res.* **2007**, *2007*, 39765.
(6) Barber, A. J. *Prog. Neuro-Psychopharmacol. Biol. Psychiatry* **2003**, *27*, 283–90.
(7) Toda, N.; Nakanishi-Toda, M. *Prog. Retinal Eye Res.* **2007**, *26*, 205–38.
(8) Park, S. H.; Kim, J. H.; Kim, Y. H.; Park, C. K. *Vision Res.* **2007**, *47*, 2732–40.
(9) Evereklioglu, C.; Er, H.; Doganay, S.; Cekmen, M.; Turkoz, Y.; Otlu, B.; Ozer, E. *Documenta Ophthalmologica* **2003**, *106*, 129–36.
(10) Marzinzig, M.; Nussler, A. K.; Stadler, J.; Marzinzig, E.; Barthlen, W.; Nussler, N. C.; Beger, H. G.; Morris, S. M.; Bruckner, U. B. *Nitric Oxide* **1997**, *1*, 177–89.
(11) Miyado, T.; Tanaka, Y.; Nagai, H.; Takeda, S.; Saito, K.; Fukushi, K.; Yoshida, Y.; Wakida, S.; Niki, E. *J. Chromatogr., A* **2004**, *1051*, 185–91.
(12) Gao, L.; Pulido, J. S.; Hatfield, R. M.; Dundervill III, R. F.; McCannel, C. A.; Shippy, S. A. *J. Chromatogr., B* **2007**, *847*, 300–4.
(13) Gao, L.; Barber-Singh, J.; Kottegoda, S.; Wirtshafter, D.; Shippy, S. A. *Electrophoresis* **2004**, *25*, 1264–9.
(14) Diederen, R. M. H.; La Heij, E. C.; Deutz, N. E. P.; Kessels, A. G. H.; van Eijk, H. M. H.; Hendriske, F. *Graefe's Arch. Clin. Exp. Ophthalmol.* **2006**, *244*, 683–8.
(15) Oku, H.; Kida, T.; Sugiyama, T.; Hamada, J.; Sato, B.; Ikeda, T. *Retina* **2001**, *21*, 647–51.

10.1021/ac800238d CCC: $40.75
Published on Web 06/13/2008

may be complicated by the highly diffusive ($D = 3300\ \mu m^2/s$)[16] nature of the substrate, NO, as well as its metabolites. To properly assay the metabolite, it was necessary to choose an in vivo sampling device capable of precise positioning and sampling from selective regions. Exact placement will aid in determining a correlation between the presence of the stable metabolite and the source of NO production in the mammalian vitreous cavity.

The use of small rodents for ophthalmologic research allows easy experimental manipulation and lower costs for husbandry. Due to the anatomically complex structure of the rat vitreous cavity, in vivo sampling from the VRI and posterior chamber poses an interesting analytical challenge. The target regions in this study are located along the inner hemispherical surface of the retina. Sampling from this area in a rat is further complicated by the small eye size (4−8-mm diameter) and relatively large lens (≥4-mm diameter) in the posterior chamber.[17] While one study has employed microdialysis for vitreal fluid collection from rats,[18] most ocular studies involving microdialysis utilize rabbits because of the larger posterior segment.[19] Certain drawbacks of microdialysis are limiting toward the study of vitreal fluids from smaller vertebrates. The size of microdialysis probes, which can extend beyond 1 mm, and relatively large guide needles (20−25 gauge), limits the degree of achievable spatial resolution as well as precise positioning in vitreous cavity.[19,20] Recently, an alternative sampling method was developed and optimized in our laboratory. Low-flow push−pull perfusion (LFPPP) allows direct infusion of physiological saline to an extracellular sampling region with simultaneous sample collection via a miniaturized sample probe.[13,21] This technique was further modified by reducing the dimensions of the probe size for rat vitreous and VRI sampling.[22] LFPPP offers several advantages compared to other available sampling methods. Using low flow rates of 50 nL/min coupled with the small probe size minimizes the amount of tissue damage, increases collection efficiencies, and affords high spatial resolution.[22] Furthermore, neurochemicals are directly collected from the region surrounding the micrometer-size tip (sampling area <0.023 mm^2) as analytes diffuse from the sampling area into the perfusion solution.[13,21,22]

Since submicroliter-volume samples are collected with LFPPP, it was necessary to choose a compatible method to concurrently assay NO_3^- and NO_2^-. Methods such as the Greiss method,[23,24] high-performance ion chromatography,[25,26] gas chromatography−mass spectrometry,[24] and high-performance liquid chromatography[27,28] have been previously described to detect NO_3^- and NO_2^-. However, shortcomings such as extensive treatment with other agents, as well as required sample volumes and analysis time, make them undesirable candidates for the small volumes generated by LFPPP. Capillary electrophoresis (CE) has been reported in the simultaneous assay of NO_3^- and NO_2^- in biological samples such as human serum and urine,[29–33] saliva,[34,35] human vitreous,[12] rat brain perfusates,[13] rat neuronal and liver tissue,[36,37] and single neurons.[38] Additionally, capillary electrophoretic assays for analyzing nitrate and nitrite in environmental samples such as river water[39,40] and sour gas[40] have been developed. CE has been coupled with UV detection,[12,13,29–32,34–36] indirect UV detection,[39–41] conventional conductivity detection,[37,38] and contactless conductivity detection[33] yielding a range of separation conditions, sensitivities, and attainable detection limits for both nitrate and nitrite. Recently, optimized CE conditions for efficiently separating NO_3^- and NO_2^- in various biological systems such as rat extracellular central nervous system (CNS) fluid in fewer than 3 min were developed in our laboratory.[13] A further modified run buffer was applied in the clinical analysis of human vitreous.[12] Such a rapid separation allows for multiple analyses of a single sample within the time it takes to collect a 0.5-μL perfusate.

The objective of this study was to assess the presence of nitrate in a region-selective manner in various domains of the rat vitreous cavity and determine whether an asymmetric composition exists with such a highly diffuse molecule. The sampling probe tip was positioned along the VRI at the optic nerve head (ONH) or in areas 1−2-mm peripheral to the optic nerve head (PONH). Additionally, the probe tip was placed in the middle vitreous (MV) area at least 1 mm from the VRI to explore possible perfusate level differences based on the source of sample collection. Markedly, assaying the vitreal fluid in positions less than 2 mm in proximity demonstrated a statistical difference ($P < 0.05$) in the presence of nitrate. The LFPPP technique was then further applied to monitor the effects of a physiological process, aging, on the presence of nitrate in the vitreous cavity. A statistically significant ($P < 0.05$) increase was observed in the mean nitrate

(16) Malinski, T.; Taha, Z.; Grunfeld, S.; Patton, S.; Kapturczak, M.; Tomboulian, P. *Biochem. Biophys. Res. Commun.* **1993**, *193*, 1076–82.
(17) Hughes, A. *Vision Res.* **1979**, *19*, 569–79.
(18) Katayama, K.; Ohshima, Y.; Tomi, M.; Hosoya, K. *J. Neurosci. Methods* **2006**, *156*, 249–56.
(19) Rittenhouse, K. D.; Pollack, G. M. *Adv. Drug Delivery Rev.* **2000**, *45*, 229–41.
(20) Macha, S.; Mitra, A. K. *Exp. Eye Res.* **2001**, *72*, 289–99.
(21) Kottegoda, S.; Shaik, I.; Shippy, S. A. *J. Neurosci. Methods* **2002**, *121*, 93–101.
(22) Kottegoda, S.; Pulido, J. S.; Thongkhao-on, K.; Shippy, S. A. *Mol. Vision* **2007**, *13*, 2073–82.
(23) Tsikas, D. *J. Chromatogr., B* **2007**, *851*, 51–70.
(24) Romitelli, F.; Santini, S. A.; Chierici, E.; Pitocco, D.; Tavazzi, B.; Amorini, A. M.; Lazzarino, G.; Di Stasio, E. *J. Chromatogr., B* **2007**, *851*, 257–67.
(25) Gapper, L. W.; Fong, B. Y.; Otter, D. E.; Indyk, H. E.; Woollard, D. C. *Int. Dairy J.* **2004**, *14*, 881–7.
(26) Smith, C. C.; Stanyer, L.; Betteridge, D. J. *J. Chromatogr., B* **2002**, *779*, 201–9.
(27) Jobgen, W. S.; Jobgen, S. C.; Li, H.; Meininger, C. J.; Wu, G. *J. Chromatogr., B* **2007**, *851*, 71–82.
(28) Di Matteo, V.; Esposito, E. *J. Chromatogr., A* **1997**, *789*, 213–9.
(29) Bories, P. N.; Scherman, E.; Dziedzic, L. *Clin. Biochem.* **1999**, *32*, 9–14.
(30) Miyado, T.; Nagai, H.; Takeda, S.; Saito, K.; Fukushi, K.; Yoshida, Y.; Wakida, S.; Niki, E. *J. Chromatogr., A* **2003**, *1014*, 197–202.
(31) Miyado, T.; Tanaka, Y.; Nagai, H.; Takeda, S.; Saito, K.; Fukushi, K.; Yoshida, Y.; Wakida, S.; Niki, E. *J. Chromatogr., A* **2006**, *1109*, 174–8.
(32) Hirokawa, T.; Yoshioka, M.; Okamoto, H.; Timerbaev, A. R.; Blaschke, G. *J. Chromatogr., B* **2004**, *811*, 165–70.
(33) Wan, Q. J.; Kubán, P.; Tanyanyiwa, J.; Rainelli, A.; Hauser, P. C. *Anal. Chim. Acta* **2004**, *525*, 11–6.
(34) Gáspár, A.; Juhász, P.; Bágyi, m K. *J. Chromatogr., A* **2005**, *1065*, 327–31.
(35) Tanaka, Y.; Naruishi, N.; Fukuya, H.; Sakata, J.; Saito, K.; Wakida, S. *J. Chromatogr., A* **2004**, *1051*, 193–97.
(36) Szöko, E.; Tábi, T.; Halász, A.; Pálfi, M.; Magyar, K. *J. Chromatogr., A* **2004**, *1051*, 177–83.
(37) Boudko, D. Y.; Cooper, B. Y.; Harvey, W. R.; Moroz, L. L. *J. Chromatogr., B* **2002**, *774*, 97–104.
(38) Moroz, L. L.; Dahlgren, R. L.; Boudko, D.; Sweedler, J. V.; Lovell, P. *J. Inorg. Biochem.* **2005**, *99*, 929–39.
(39) Barciela Alonso, M. C.; Prego, R. *Anal. Chim. Acta* **2000**, *416*, 21–7.
(40) Hiissa, T.; Siren, H.; Kotiaho, T.; Snellman, M.; Hautojärvi, A. *J. Chromatogr., A* **1999**, *853*, 403–11.
(41) Bord, N.; Cretier, G.; Rocca, J. L.; Bailly, C.; Souchez, J. P. *J. Chromatogr., A* **2005**, *1100*, 223–9.

level in the mature animals that may be associated with the aging process as well as an increase in body mass.

EXPERIMENTAL SECTION

Chemicals and Reagents. Calcium chloride, magnesium chloride, sodium phosphate, sodium monobasic phosphate, sodium citrate, citric acid, and NG-nitro-L-arginine methyl ester hydrochloride (L-NAME) (99%) were purchased from Fisher Scientific (Itasca, IL). Potassium chloride, sodium chloride, cetyltrimethylammonium chloride (CTAC), sodium nitrate (≥99.0%), and sodium nitrite (≥99.0%) were obtained from Sigma-Aldrich (St. Louis, MO). Proparacaine hydrochloride, gentamicin sulfate, and tropicamide were obtained from Akorn (Buffalo Grove, IL). The composition of the Krebs-Ringer buffer (KRB) was 3 mM KCl, 145 mM NaCl, 1.2 mM $CaCl_2$, 1 mM $MgCl_2$, 1.61 mM Na_2HPO_4, 0.4 mM NaH_2PO_4, and 0.2 mM ascorbic acid (pH 7.5). Optimized separation buffer consisted of 150 mM NaCl and 2 mM CTAC with the pH adjusted to 3.5 by 5 mM sodium citrate and citric acid.[12] All solutions, unless stated otherwise, were prepared in deionized water from a US Filter Purelab Plus water purification system (Lowell, MA) and filtered with 0.22-μm Millex GP filters purchased from Millipore Corp. (Bedford, MA). Nitrate and nitrite standard solutions were prepared in KRB. Cyanoacrylate-based sealant (Loctite) was purchased from Small Parts Inc. (Mirimar, FL). Epoxy-based sealant (Quick Setting Epoxy Adhesive) was purchased from The Super Glue Corp. (Rancho Cucamonga, CA).

Animals. Male, Hooded-Long Evan rats weighing 300−600 g were purchased from Harlan (Indianapolis, IN). Animal protocols were approved by the University of Illinois at Chicago Institutional Animal Care and Use Committee and followed the Association for Research in Vision and Ophthalmology statement for the use of animals in ophthalmic and vision research. Rats were allowed to adapt to their controlled environment (25 °C and 12:12-h light/dark cycle) with food and water available ad libitum for at least one week prior to experimentation. Mature animals were allowed to age normally until they were between 4.5 and 8 months and weighed 420−600 g at the time of sampling.

Modified Push−Pull Probe. The push−pull probe construction procedure was described previously.[22] Briefly, the sampling probes consist of concentric fused-silica capillaries that allow direct infusion of physiological saline to the desired sampling region via an outer infusion capillary (170/100 μm o.d./i.d.) and simultaneous sample collection via an inner withdraw capillary (90/20 μm o.d./i.d.). Previous models of the brain and eye[13,22] push−pull probes were constructed using a cyanoacrylate glue.[21] However, when placed in water, this brand of glue generated a background nitrate peak in the electropherograms that would interfere with quantification. It was necessary to identify an adhesive that would generate an insignificant background peak and would effectively bond fused silica, Tygon tubing, and stainless steel. A range of adhesives, which included epoxy, silicone, and toluene/petroleum distillate glues, was used to construct the eye probes. The toluene/petroleum distillate glue was not effective in sealing all materials together. The epoxy and silicon adhesives were capable of binding the materials together. However, after a series of in vitro experiments, which involved collecting KRB through constructed probes and nitrate analysis, it was determined that the epoxy adhesive provided the least significant and most consistent background peak. Because there was still a minor peak generated, it was necessary to correct the perfusate values by performing background subtraction.

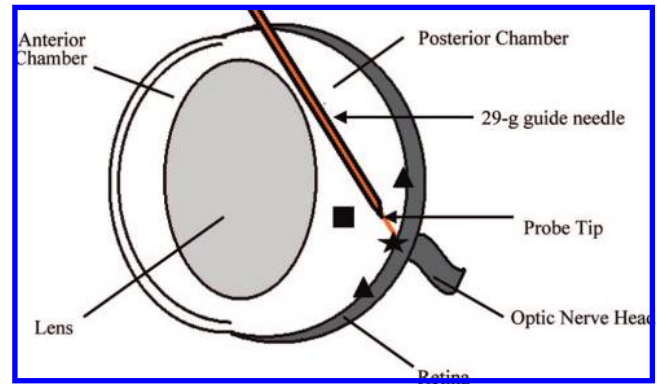

Figure 1. Schematic of placement of sampling probe in vitreous cavity (cross-section view). A 29-gauge needle was inserted through the sclera into the posterior chamber. The needle was then directed toward the desired sampling position. The push−pull probe was inserted at a high flow rate to avoid occlusion of the probe tip. Sampling positions: (▲) PONH, (■) MV, and (★) ONH.

Background Nitrate Subtraction. Prior to in vivo sampling, in vitro sampling with KRB utilizing the same probe was performed in which eight samples were collected. The average peak height present in vitro was then subtracted from each of the collected perfusate values. To confirm that the background subtraction method would provide a definitive correlation between the nitrate level in the perfusates and the displayed signal, an additional test where KRB and standard nitrate solutions were withdrawn from a bare, 15-cm segment of 365/20 μm (o.d./i.d.) silica capillary was conducted. KRB and standard solutions were assayed prior to flow through the capillary and after the withdraw process that simulated the actual sampling procedure. The average peak height observed in the KRB sample after being withdrawn was subtracted from the standard solution signal after being collected.

Animal Preparation and Sample Collection. Animals were deeply anesthetized with an intraperitoneal (ip) injection of 50 mg/kg sodium pentobarbital and were administered additional doses (10 mg/kg) to sustain anesthesia in response to a reflex generated by a tail pinch. After the head of the subject was stabilized in a stereotaxic apparatus, 0.05% proparacaine hydrochloride (1:10 dilution with KRB) was applied dropwise every 5−10 min throughout the procedure to minimize the blink reflex. The pupil was dilated by applying 1% tropicamide solution dropwise 10−15 min prior to guide needle insertion. Once the pupil was dilated to encompass >80% of the cornea and the optic nerve head and retina were completely visible, a 29-gauge guide needle was inserted into the posterior segment through the conjunctiva and sclera at the extreme peripheral retina. The needle was directed toward different positions on the VRI by adjusting the coordinates on the stereotaxic apparatus. The target locations are represented in Figure 1. Complete dilation and proper positioning were verified visually by indirect opthalmoscopy and a 60 diopter condensing lens. The probe was then inserted through the guide at a high flow rate of 500 nL/min to prevent occlusion of the tip during placement. Upon insertion, the flow rate was decreased linearly to 45−50 nL/min and allowed to stabilize for 5−10 min. The sampling probe extends 1 mm beyond the bevel of the guide

needle in order to serve as a measure of distance and to aid in precise probe positioning. The guide needle and probe tip were positioned carefully until the tip barely touched the retinal surface (ONH or PONH sampling) or until it was at least 1 mm from the retina for MV sampling. KRB was pushed into the infusion capillary with a PHD 2000 programmable syringe pump (Harvard Apparatus, Holliston, MA). Concurrently, 0.5-μL samples were withdrawn by an inner-withdrawing capillary into a 4-cm-long, 250-μm-i.d. Tygon tubing every 10 min by lowering the pressure below atmosphere using a vacuum pump (Barnant Co., Barrington, IL) and regulator. The Tygon tubing was typically replaced within 30−45 s. The total sampling time was up to 2.5 h. Collected samples were stored in sealed, 0.25-mL centrifuge tubes until analysis. After sampling, a drop of 0.3% gentamicin sulfate was administered to the eye prophylactically. The animals were given a recovery period of 1 week before subsequent studies were performed on the fellow eye. Five different subjects were utilized for each of the target locations and the maturation study.

To determine that the observed nitrate signal was the result of NOS activity, 60 min after beginning sample collection, the infusion line was switched from a KRB solution to a KRB solution with 5 mM L-NAME, a nonselective inhibitor of NOS, for 30 min. After the 30-min time frame, the infusion line was transferred back to the syringe containing only KRB to determine the effect on the nitrate signal post inhibitor administration.

Electrophoretic Assay. Separation conditions were previously optimized in our laboratory for assaying nitrate and nitrite simultaneously in rat brain perfusates[13] and for clinical vitreous samples.[12] Briefly, electrophoretic assays were performed on a laboratory-built CE system with a commercial high-voltage supply (Spellman, NY) and a VUV-20 variable-wavelength ultraviolet/visible absorbance detector (Hyperquan, CO). All separations were achieved in 360/75 μm o.d./i.d. fused-silica capillary (Polymicro Technologies) with a total length of 40 cm (22 cm effective) at an applied negative voltage of 5 kV. The CE capillary, buffer vials, and electrode assembly were placed in a plexiglass box to isolate these components and protect the operator from the high voltage. Before use, new capillaries were conditioned with deionized water followed by 0.1 M NaOH, deionized water, and finally separation buffer at intervals of 30−60 s each. Samples were injected gravimetrically at 10 cm for 10 s allowing ~7 nL to be transferred to the capillary. Consecutive injections were performed from the same sample vial. Absorbance measurements ($\lambda = 214$ nm) were recorded in text format at a frequency of 10 Hz using a custom LabVIEW (National Instruments, TX) data acquisition program.

Data Analysis. Raw data were exported from a custom LabVIEW data acquisition program to Microsoft Excel in order to plot electrophoretic data. Peak heights were measured from electropherograms by subtracting the baseline, which was considered to be the average signal 2 s after the nitrate peak and 2 s before the nitrite peak, from the peak maximum. The noise was calculated as the standard deviation of the same baseline section of the electropherogram. The signal-to-noise ratio (S/N) was calculated from the peak height divided by the standard deviation of the baseline. Concentrations were derived from constructed in vitro calibration curves.

Statistical calculations were performed in Excel. An *F*-test was first used to determine whether standard deviations from each region were significantly different. Statistical significance was then determined by calculation of a Student's *t*-test at the 95% confidence level. Unpaired, homoscedastic or heteroscedastic *t*-test was chosen according to previous *F*-test results. Results are represented as mean ± standard deviation.

RESULTS AND DISCUSSION

Optimization of Push−Pull Probe and in Vitro Percent Recovery. Earlier versions of the sampling probes utilized a cyanoacrylate-based glue to bond all materials together; however, in vitro studies revealed that this particular sealant may leach nitrate, thus causing a rather high and inconsistent background nitrate peak. The Materials Safety Data Sheet (MSDS) also revealed that cyanoacrylate is slightly soluble in water. To resolve this problem, it was necessary to identify an appropriate water-insoluble sealant that would produce a negligible background peak. It was determined through a series of in vitro experiments that an epoxy-based sealant provided the least significant background nitrate peak. A representative electropherogram of the background NO_3^- peak obtained from the two different sealants is provided in Figure 2A. Upon additional examination, it is believed that the background nitrate peak may also be partially associated to a concentrating effect related to the surface of the smaller i.d. capillary that was not seen in larger i.d. capillaries. Further in vitro experiments where both KRB and ultrafiltered deionized water were withdrawn through bare silica (365/20 μm o.d./i.d. and 360/50 μm o.d./i.d.) capillaries demonstrated a problematic nitrate peak in the smaller capillary electropherogram that was not present prior to withdrawal. This peak was not observed in the larger capillary electropherogram (see Figure 2B). A background subtraction method was developed and tested on a range of standard nitrate solutions. The results are provided in the inset of Figure 2B. This method demonstrates that there is no significant ($P > 0.05$) difference between the corrected peak height and peak height of the original solution for a range of concentrations ($n = 3$). While absolute recoveries and basal level determination may be affected by this system peak, the consistency demonstrates that relative levels may be read unambiguously. In vitro testing for collection efficiency using standard 30 μM nitrate/nitrite solution with a flow rate of 50 nL/min determined recoveries of 46.4 ± 9.5 and 71.0 ± 12.3%, respectively, for nitrate and nitrite ($n = 4$) for the eye probes. There is a ~3-fold increase in percent recovery of nitrate and a ~6-fold increase for nitrite compared to previous in vitro experiments with microdialysis probes conducted at a flow rate of 2 μL/min (16.4 and 12.4%, for nitrate and nitrite, respectively).[42]

LFPPP Sampling. The purpose of this study was to simultaneously assay the level of NO metabolites, primarily nitrate, at specific sites located in the posterior chamber of the rat eye. Two important parameters that need to be considered when choosing an appropriate site-specific, in vivo sampling tool capable of collecting perfusates from the rat vitreous cavity are the location of the target regions along the hemispherically shaped VRI in addition to the small dimensions of the eye. The miniaturized probe construction of LFPPP is capable of being positioned

(42) Gao, L. Capillary Electrophoretic Assays for Nitric Oxide Metabolites from Low Volume Biological Samples. Ph.D. Dissertation, University of Illinois at Chicago, 2007.

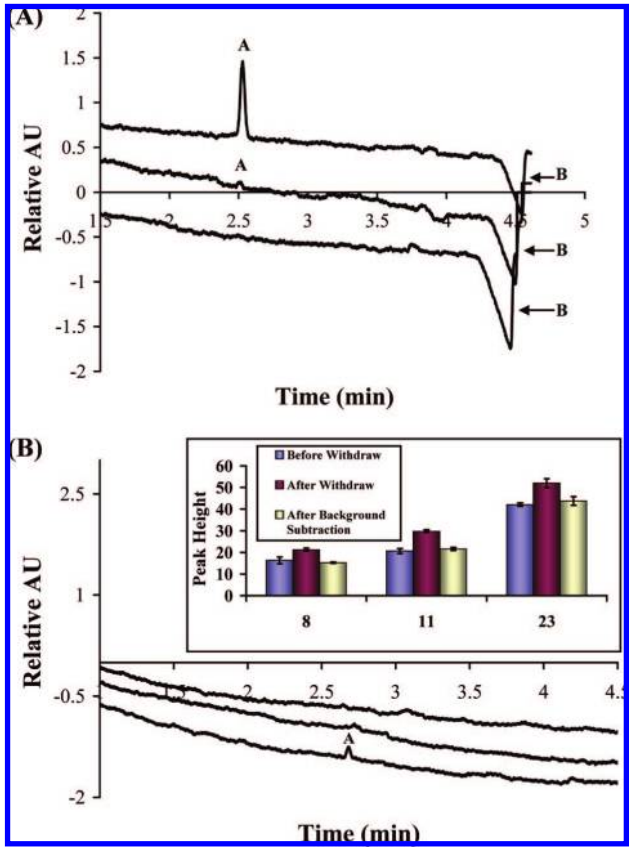

Figure 2. (A) Representative electropherograms of background nitrate peak seen in in vitro perfusates. Top to bottom: electropherogram for cyanoacrylate probe, epoxy probe, and blank (KRB). Peak A identifies the nitrate signal produced from the probe. Peak B corresponds to the chloride peak that corresponds to ~0.15 M Cl^- level. Separation conditions: 5 kV (negative polarity), 40 cm × 75 μm (i.d.) (22 cm effective), −125 V/cm, λ = 214 nm, 10-s gravity injection at 10 cm. Run buffer: 150 mM NaCl, 5 mM sodium citrate/citric acid, 2 mM CTAC, pH ~3.5. (B) Representative electropherograms of ultrafiltered deionized water before and after being withdrawn through bare silica capillaries. Top to bottom: electropherogram for water before being withdrawn, after withdrawal through a large capillary (360/50 μm (o.d./i.d.)), and after withdrawal though a small capillary (365/20 μm (o.d./i.d.)). Peak A corresponds to the nitrate signal. Inset: background nitrate subtraction. KRB and standard nitrate solutions were assayed using the same separation conditions as in (A) prior to withdraw via a bare, 365/20 (o.d./i.d.) capillary and afterward. The average peak height observed in the KRB sample was subtracted from the signal obtained from each of the solutions after the withdraw procedure (n = 3).

precisely in the rat posterior chamber while minimally perturbing the retina. A representation of the push−pull probe placed in the posterior segment and the target sampling locations are provided in Figure 1. Recently, our laboratory has reported basal levels for 10 amino acids at the rat VRI and in the middle vitreous region using LFPPP.[22] Notably, there was no significant difference in basal amino acid concentration in perfusates collected along the VRI or from the middle vitreous region. We have previously applied LFPPP to submicroliter sample collection from the rat vitreous cavity; therefore, the main emphasis of this work was to characterize the presence of nitrate with respect to the site where perfusates were collected in the posterior chamber during a specified time interval.

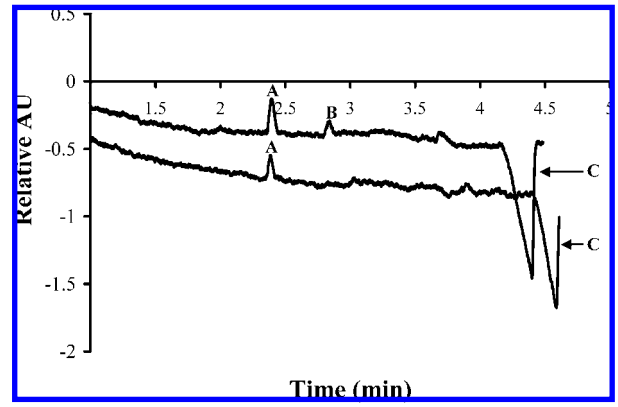

Figure 3. Representative electropherogram of nitrate and nitrite analysis. The bottom electropherogram represents a typical perfusate separation. The top electropherogram represents the same perfusate spiked with a standard 40 μM nitrate/nitrite solution. Identified peaks correspond to (A) nitrate, (B) nitrite, and (C) chloride. Separation conditions are the same as in Figure 2.

NO Metabolite Assay. In the present study, collected perfusates from the vitreous cavity were obtained by LFPPP over a 2−2.5-h period. Each sample collected at a fixed interval (10 min) represents an average NO metabolite concentration obtained during that specific period. The perfusates were analyzed for NO metabolites using CE-UV. A representative electropherogram of a rat vitreous perfusate with and without a standard nitrate/nitrite solution spike are shown in Figure 3 at optimized conditions. Total separation of nitrate and nitrite was achieved in fewer than 3 min. With such a rapid separation, multiple analyses of a single sample can be performed within the time it takes to collect one perfusate. Nitrate and nitrite are well resolved from each other as well as from the chloride peak. This is necessary because biological samples have relatively high chloride content (>150 mM) that may interfere with proper quantification of nitrate.[10] The chloride peak is negative due to less chloride in the sample solution compared with total chloride present in the run buffer from 150 mM NaCl and 2 mM CTAC.[12] The NO_2^- peak was not consistently observed in individual subjects, and its concentration in vitreous perfusates is likely below our limit of detection (LOD). Methods such as transient isotachophoresis (tITP) or field-amplified sample stacking (FASS) could possibly improve the LOD for both analytes. However, previous data have suggested that NO_3^- is the major metabolite of NO;[43,44] therefore, quantification was solely based upon NO_3^-.[12]

In vivo perfusate levels were monitored continuously, and concentrations were derived from an in vitro calibration curve prepared from standard solutions of nitrate and nitrite at various concentrations (2.5−40.0 μM). The regression equations were as follows: $y = 1.94x + 4.89$ ($R^2 = 0.996$) for nitrate and $y = 0.885x + 2.81$ ($R^2 = 0.997$) for nitrite where the x-value is analyte concentration (μM) and the y-value is absorbance. With these regression equations, the LOD of nitrate was determined to be 3.65 μM, and 10.8 μM for nitrite, based on a S/N = 3. Previous reports have utilized stacking techniques such as tITP[32,36,45,46]

(43) Tsikas, D. *Free Radical Res.* **2005**, *39*, 797–815.
(44) Sagnella, G. A.; Markandu, N. D.; Onipinla, A. K.; Chelliah, R.; Singer, D. R. J.; MacGregor, G. A. *J. Hum. Hypertens.* **1997**, *11*, 587–8.
(45) Fukushi, K.; Nakayama, Y.; Tsujimoto, J. *J. Chromatogr., A* **2003**, *1005*, 197–205.

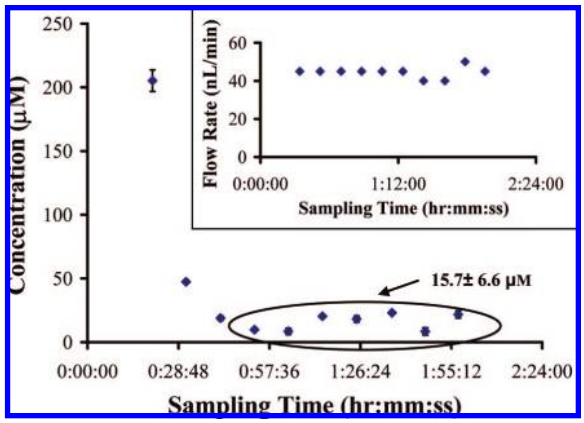

Figure 4. Average perfusate nitrate concentration values (error bars ± std dev) versus sampling time for one subject. A similar trend was observed in all subjects. Samples were collected from the ONH region. Each sample was analyzed in triplicate, and a concentration was determined using a constructed calibration curve. Average perfusate value for subject is enclosed in the circle. Inset: flow rate (nL/min) versus sampling time.

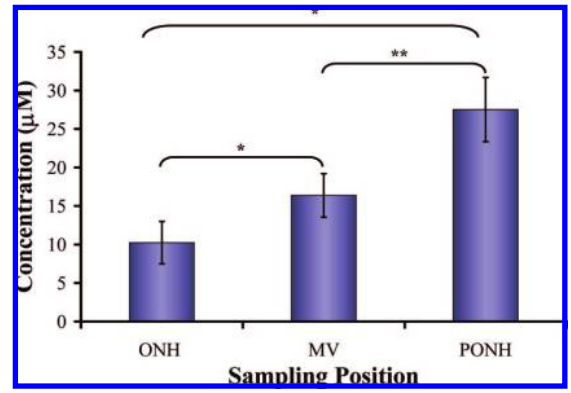

Figure 5. Average nitrate concentrations for ONH, MV, and PONH (10.3 ± 2.8, 16.4 ± 2.8, and 27.5 ± 4.2 μM, respectively) ($n = 5$ for each location). Nitrate concentration at the MV and PONH were significantly higher compared to the ONH (*$P < 0.05$). Additionally, nitrate concentration at the PONH was significantly higher than MV (**$P < 0.05$). These results have not been corrected for percent recovery.

and FASS[36,47] to improve LODs for both nitrate and nitrite. While this enhancement would be beneficial in quantifying both metabolites, these processes typically employ injecting larger sample plugs into the capillary. The submicroliter volume of individual vitreous perfusates collected makes the use of tITP difficult and would limit the number of repeated injections from a single sample reducing the accuracy of the determination. Sample stacking with FASS can afford improvements,[48] but there was only a slight increase in the nitrite peak obtained.[46,49,50] Further, the use of FASS can increase the amount of time per sample run greater than 33%. This is an undesirable tradeoff for the nature of this work for the limited nitrite peak improvement.

Since samples were collected every 10 min, 10−12 perfusates were afforded from the entire sampling process. Samples were analyzed in triplicate and averaged concentration values for each sample were plotted against sampling time. A representative plot of averaged perfusate values plotted against time is shown in Figure 4. A similar trend was observed in all subjects. Initial NO_3^- levels were likely high due to the insertion of the guide needle;[13] therefore, the basal concentration of nitrate was considered perfusate values corresponding to samples collected during 30−150 min of sampling as the signal leveled off during this period. Ideally, the flow rate should remain consistent throughout the time course of the experiment; however, a decrease may be seen during the end of the experiment (inset of Figure 4). This is likely due to adhesion of the viscous solution to the capillary wall. To alleviate this, the pressure can be lowered and the infusion flow rate can be increased to resume a desired flow rate.

Nitrate Analysis in Rat Vitreous Perfusates. We evaluated the application of LFPPP for the continuous collection of nitrate from the rat vitreous cavity. Significantly different nitrate concentrations were obtained from three different regions that were within 1−2 mm to each other: ONH, PONH, and MV (Figure 1). The average perfusate levels are represented in Figure 5 and are reported without correction for percent recovery ($n = 5$ for all sampling locations). The basal levels for the ONH, MV, and PONH are 10.3 ± 2.8, 16.4 ± 2.8, and 27.5 ± 4.2 μM, respectively. Clinical studies have reported vitreal NOx (nitrate + nitrite; predominantly nitrate) ranging from 15.22 ± 0.86 to 24.2 ± 2.8 μM in control subjects based on either a capillary electrophoretic assay[12] or the Griess reaction[15,51,52] which are comparable to our MV and PONH values. An in vivo dialysate value of nitrate at the rabbit ONH that was assessed using the Griess reaction has been reported at 3.95 ± 0.50 μM.[53] This value is much lower than our reported observation at the rat ONH; however, this difference is likely due to the lower recoveries obtained by microdialysis, the method of nitrate assessment (Griess reaction vs electrophoretic assay), and the type of animal model employed. The location of the PONH and MV regions can be approximated with respect to the ONH by the 1-mm-long probe tip that extends beyond the guide needle. For VRI sampling, the probe tip was positioned to barely graze the retinal plane and there was a 1−2-mm separation between the ONH and PONH regions. For MV sampling, the probe and guide needle were positioned posterior to the lens and at least 1 mm away from the retinal surface. The site-specific placement of the push−pull probe demonstrated that the mean nitrate value was statistically increased in both the PONH ($P < 0.0001$) and MV ($P < 0.01$) compared to the mean value observed in the ONH. Additionally, the mean value of nitrate in the MV region was significantly lower than the PONH ($P < 0.001$) region. NO and nitrate are a freely diffusing molecules; however, we have observed an asymmetric pattern of nitrate levels at various regions in the posterior chamber. We have previously demonstrated the degree of spatial resolution obtained by LFPPP by monitoring retinal

(46) Tu, C.; Lee, H. K. *J. Chromatogr., A* **2002**, *966*, 205–12.
(47) Timerbaev, A. R.; Fukushi, K.; Miyado, T.; Ishio, N.; Saito, K.; Motomizu, S. *J. Chromatogr., A* **2000**, *888*, 309–19.
(48) Breadmore, M. C.; Haddad, P. R. *Electrophoresis* **2001**, *22*, 2464–89.
(49) Fukushi, K.; Ishio, N.; Sumida, M.; Takeda, S.; Wakida, S.; Hiiro, K. *Electrophoresis* **200**, *21*, 2866–71.
(50) Fukushi, K.; Miyado, T.; Ishio, N.; Nishio, H.; Saito, K.; Takeda, S.; Wakida, S. *Electrophoresis* **2002**, *23*, 1928–34.
(51) Cicik, E.; Tekin, H.; Akar, S.; Ekmekci, O.; Donma, O.; Koldas, L.; Ozkan, S. *Ophthalmic Res.* **2003**, *35*, 251–5.
(52) Hernandez, C.; Lecube, A.; Segura, R. M.; Sararols, L.; Simo, R. *Diabetic Med.* **2002**, *19*, 655–60.
(53) Okuno, T.; Oku, H.; Sugiyama, T.; Goto, W.; Ikeda, T. *Ophthalmic Res/* **2003**, *35*, 78–83.

tissue responses to an infused drug.[22] The differences seen here are somewhat surprising but are likely due to attention to the precise positioning of the push−pull probe.

Our results suggest that the extent of NO production likely varies with the location in the posterior chamber. NO is generated from L-arginine by the nitric oxide synthase (NOS) enzymatic family, with formation of L-citrulline as a co-product.[54] Three different isoforms of NOS exist; two of which are constitutively expressed and are Ca^{2+} dependent (endothelial, eNOS and neuronal, nNOS) and one which is induced by immunological signals due to sustained tissue damage (inducible, iNOS)[2] that is present in diseased states such as diabetic retinopathy.[55] Immunohistochemical staining evidence has suggested asymmetric localization of different NOS isoforms across the retina.[54] Although not examined in detail, the optic nerve axons are essentially absent of NOS activity in control rats according to the report of Yamamoto et al. Further experimentation revealed that it was possible to surgically induce Ca^{2+}-dependent NOS activity at the ONH; however, they were unable to identify the enzyme as being the neuronal or endothelial form of NOS.[56] Additionally, it has been reported that constitutive isoforms, predominantly nNOS, localize in retinal neurons and peripheral nerve fibers.[54,56] This evidence strongly supports our findings of ~3-fold higher mean levels of nitrate in the PONH compared to the ONH. However, Shareef et al. have reported immunohistochemical data suggesting nNOS and eNOS staining associated with the vasculature regions of the ONH. They also suggested that the iNOS form is mainly associated with neurotoxicity and can be induced under ischemic conditions.[57] While these results seem contradictory to what Yamamoto reported, it suggests that constitutive isoforms are present across the retinal surface at different levels depending on the location. NO production may vary due to the relative contribution of the nNOS, eNOS, and iNOS isoforms. This variation in NOS expression would likely result in a difference in NO production, thus, leading to a difference in the presence of its major metabolite, nitrate, at each of the different positions tested here. Despite the conflicting reports, our results clearly show a significant difference in the presence of NO_3^- along the VRI and in the vitreous cavity.

NOS inhibitors may be delivered directly to specific regions via the push−pull probe similar to our previous study of amino acids[22] and their effects on the presence of nitrate can be examined through time. As a first step to explore the relationship between NOS activity and the observed nitrate levels, a control experiment in which a nonselective NOS inhibitor, L-NAME, was infused through the push−pull probe to the PONH area was designed. Upon delivering the inhibitor, there was a significant decrease ($P < 0.05$) after 20 min in the observed nitrate level (Figure 6; $n = 3$). The nitrate signal was reduced to 65% of the baseline. During the last 10 min of drug infusion and once KRB infusion resumed, the nitrate level appears to return to baseline values. The data demonstrate that the nitrate level measured is directly related to NOS activity. Similar to our previous results, a region of the retina can be pharmacologically manipulated by inclusion of the drug into the perfusion solution. Further studies using selective and nonselective NOS inhibitors will be conducted to more clearly define the in vivo activity and localization of the NOS isoforms.

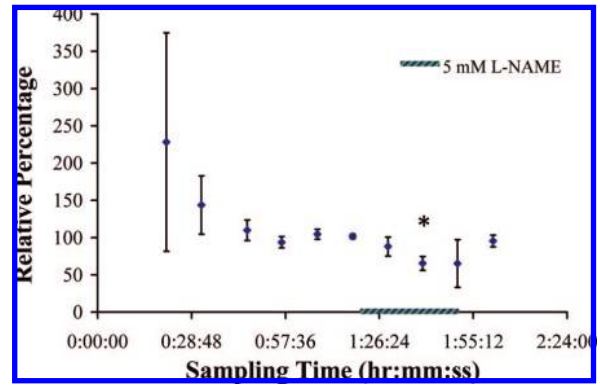

Figure 6. L-NAME infusion. Average perfusate nitrate concentration expressed as % baseline levels for 3 subjects. Samples 4−6 were used to establish baseline levels (100%), and reported values were expressed as % baseline. The observed nitrate signal decreases to ~65% of baseline during the second 10-min interval of drug infusion (*$P < 0.05$).

Table 1. Nitrate Concentration at the Optic Nerve Head, Age Range, and Body Weight of Control and Mature Subjects

	age range (months)	body weight (g)	perfusate nitrate (μM)
control: ONH	2−3.5	374 ± 18	10.3 ± 2.8
mature: ONH	4.5−8	512 ± 71	30.3 ± 6.5
		P-value: 0.002	*P*-value: 0.0001

In addition to the asymmetric NO production theory, we also postulate that the clearance mechanism of NO and its metabolites from the vitreous cavity may be responsible for the asymmetric presence of NO_3^-. Our observed NO_3^- pattern may suggest homogeneous NO production across the VRI and the vitreous cavity with a "sink-like" removal system. The vascular network convenes at the optic nerve head, which may provide a more rapid transport of nitrate from the VRI thus resulting in a lower level of NO_3^- at the ONH compared to other regions of the vitreous cavity. It is also likely that our results are reflective of both the source of NO production and the clearance mechanism from the posterior chamber. Further exploration of these hypotheses is needed.

Application of LFPPP To Monitor Physiological Changes in Nitrate. As a further preliminary assessment of vitreoretinal nitrate levels from different physiological conditions, this study aimed to quantify NO_3^- from mature retinas that likely have different NO production or NO_3^- accumulation patterns. Subjects were allowed to mature normally until they were between 4.5 and 8 months of age at the time of sampling. The average results are reported in Table 1. Mature animal VRI perfusates displayed an approximate 3-fold increase in the mean value of nitrate (30.3 ± 6.5 μM) compared to samples collected from the same region of younger animals ($n = 5$ for both groups). This difference was found to be statistically significant ($P < 0.05$). Aging is a naturally occurring phenomenon that may be associated with the accumula-

(54) Becquet, F.; Courtois, Y.; Goureau, O. *Surv. Ophthalmol.* **1997**, *42*, 71–82.
(55) Zheng, L.; Du, Y.; Miller, C.; Gubitosi-Klug, R. A.; Kern, T. S.; Ball, S.; Berkowitz, B. A. *Diabetologia* **2007**, *50*, 1987–96.
(56) Yamamoto, R.; Bredt, D. S.; Dawson, T. M.; Snyder, S. H.; Stone; Richard, A. *Brain Res.* **1993**, *631*, 83–8.
(57) Shareef, S.; Sawada, A.; Neufeld, A. H. *Invest. Ophthalmol. Vision Sci.* **1999**, *40*, 2884–91.

tion of free radicals and neuron loss due to oxidative damage.[58] Previous reports have implicated increased production of NO, a free radical, in the CNS during the aging process.[59] Liu et al. demonstrated that there is an increase in total NOS activity in subregions of the hippocampus of aged animals (24 months).[60,61] Additionally, age-associated ocular diseases such as age-related macular degeneration have been linked with an increase of plasma NO levels.[9] Our results suggest that there is a positive relationship between maturation and the presence of the major NO metabolite in the rat vitreous cavity. To the best of the authors' knowledge, this is the first study to examine the effect of age on the presence of nitrate in the vitreous cavity. However, it is important to note that the average body weight sustained by mature animals (Table 1) was also statistically higher ($P < 0.05$) than the normal animals. A clinical study has suggested a correlation between increased NO levels and obesity.[62] The design of the study presented here does not isolate potential effects due to aging or increased body weight. Although speculative, it is possible that higher vitreoretinal nitrate levels are reflective of both age and body weight because the older animals also appear to have increased body weight. Nevertheless, the sampling method was capable of quantifying a vitreoretinal nitrate level difference between groups that might be expected to display such a difference.

CONCLUSION

In this work, we have demonstrated the possibility of describing the extracellular presence of the major NO metabolite, nitrate, in various regions in the rat vitreous cavity using LFPPP coupled with a rapid capillary electrophoretic assay. In vivo sample collection permitted the quantification of nitrate at the optic nerve head, peripheral to the optic nerve head, and the middle vitreous. There was a statistically significant difference in the presence of nitrate in the perfusates collected from each of the sampling regions. Observed nitrate levels are clearly related to NOS activity based on L-NAME infusion. This also demonstrates the ability to pharmacologically manipulate retinal tissue at the tip. It remains unclear if this difference is due to the distinct localization of the different NOS isoforms along the vitreoretinal interface or the clearance mechanism of the substrate and its metabolites. Additionally, we have shown that there is a significant elevation in the level of nitrate present at the ONH in animals that were older than 4.5 months. Further studies must be conducted in order to determine whether the increase is solely due to the aging process or whether increased body weight is an alternate factor in increased production of nitric oxide. One possible route might involve allowing the subject to age normally but enforce a calorie-restricted diet to reduce the amount of weight that would be gained. Additionally assessment of nitrate levels in older animals ($\geq$24 months) should be performed to establish if the increase is linearly related to the aging process. Understanding the source of NO in the mammalian retina and its function at various locations in the vitreous cavity may facilitate therapeutic treatments for retinal diseases associated with misregulation of NO production.

(58) McCann, S. M.; Licinio, J.; Wong, M. L.; Yu, W. H.; Karanth, S.; Rettorri, V. *Exp. Gerontol.* **1998**, *33*, 813–26.

(59) Özdemir, S.; Yargiço, P.; Agar, A.; Gümüslü, S.; Bilmen, S.; Hacioglu, G. *Int. J. Neurosci.* **2002**, *112*, 263–76.

(60) Liu, P.; Smith, P. F.; Appleton, I.; Darlington, C. L.; Bilkey, D. K. *Exp. Gerontolo.* **2004**, *39*, 1207–22.

(61) Liu, P.; Smith, P. F.; Appleton, I.; Darlington, C. L.; Bilkey, D. K. *Neuroscience* **2003**, *119*, 679–87.

(62) Choi, J. W.; Pai, S. H.; Kim, S. K.; Ito, M.; Park, C. S.; Cha, Y. N. *Clin. Chem.* **2001**, *47*, 1106–9.

ACKNOWLEDGMENT

This work was supported by the NIH grant EY014908. The authors thank Michael Ragozzino for donation of the mature animals as well as David Wirtshafter for the use of laboratory facilities for some experiments.

Received for review February 1, 2008. Accepted May 14, 2008.

AC800238D